TASK QUARTERLY 10 No 2, 191–206

# HIGH-LIFT BEHAVIOUR OF HALF-MODELS AT FLIGHT REYNOLDS NUMBERS

PIOTR DOERFFER AND OSKAR SZULC

*Institute of Fluid-Flow Machinery,*
*Polish Academy of Sciences,*
*Fiszera 14, 80-952 Gdansk, Poland*
*doerffer@imp.gda.pl*

(Received 7 March 2006)

**Abstract:** A peniche is designed to offset a half-span aircraft model from the wind tunnel wall boundary layer. This strategy of model mounting results in large influence on the measured aerodynamic coefficients, compared with full-span data. The negative influence is especially important in high-lift conditions leading to incorrect maximum lift behaviour.

A very time-consuming set of python scripts was constructed to allow automatic meshing of the wing-body configuration of the DLR F11 high-lift model placed in the European Transonic Wind tunnel (ETW, Germany). Variations due to different concepts of model mountings (peniches) were included. A block-structured FLOWer solver (DLR, Germany) was used for all flow simulations, simplifying the mesh generation process by using the chimera overlapping grids technique.

Preliminary results are available for a full-span configuration obtained with a symmetry condition at the mirror plane. Computations of the half-span model placed directly at the wall or mounted using a standard peniche are also presented.

**Keywords:** half-span, wing-body, high-lift, peniche, Navier-Stokes

## 1. Introduction

Despite considerable progress in Computational Fluid Dynamics wind tunnels are still a prime tool to measure and predict aircraft performance for take-off, landing and cruise conditions. Only pressurized cryogenic wind tunnels are suitable for tests at Reynolds numbers needed for medium- or large-sized aircraft, providing complete fluid dynamics similarity to a flying airplane. However, the interaction of supports with the model still represents a difficult problem.

Half-span models are often utilized in order to increase the achievable Reynolds numbers of the wind tunnel facilities (see Figure 1) [1–4]. Usage of half-models not only doubles the maximum Reynolds number, but also enhances the quality of the measurement data. Unfortunately, compared to full-span, half-span models mounted on a wind tunnel wall are influenced by the wall's boundary layer. An additional penalty appears at high angles of attack, where flow separation on fuselage's upper

surface is significantly greater than that of full-span models, which may influence the behaviour of the maximum lift coefficient.

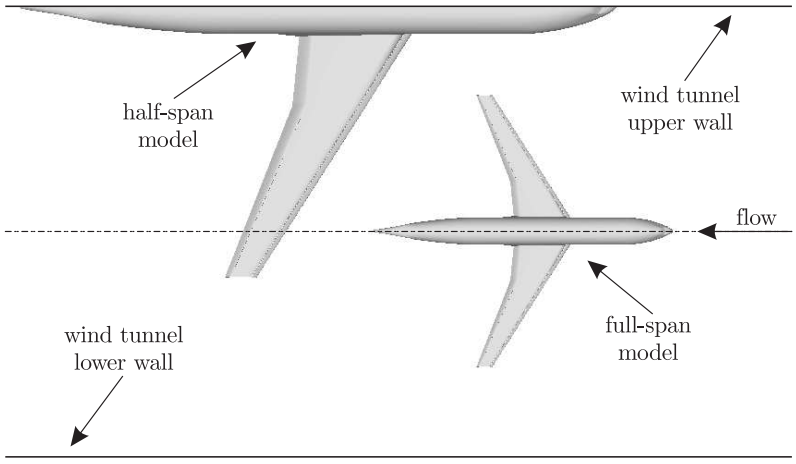


**Figure 1.** Full- and half-span models in a wind tunnel

Application of the half-model technique creates a completely new three-dimensional vortical structure, a horse-shoe vortex. In order to compensate the wall's influence, the peniche technique is applied in half-model tests. The peniche is an additional insertion between the half-fuselage and the wind tunnel wall (see Figure 2) supposed to reduce the impact of the wall boundary layer on the model flow. The simplest peniche shape is a constant profile identical to the fuselage's centreline cross-section.

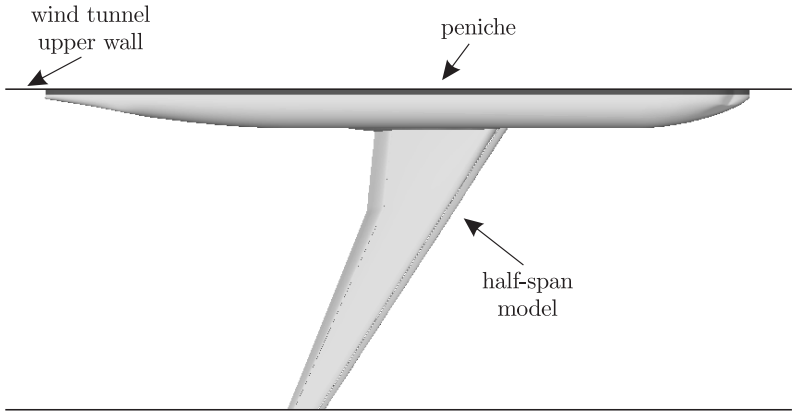


**Figure 2.** A half-span model with a peniche

The interaction between the wall boundary layer and the peniche and the resulting effects on wing aerodynamics are not well understood yet. The existing complex 3D flow behaviour suggests optimization of the peniche's height for requested test conditions, but detailed knowledge and deeper understanding of the flow phenomena of half-model testing is very important. It would allow improvements in wind tunnel correction methods of free flight prediction.

## 2. The DLR F11 model in the European Transonic Wind tunnel

The European Transonic Wind tunnel in Cologne (Germany) is a cryogenic, high pressure, high speed facility (Table 1). It provides the capability for achieving full-scale Reynolds numbers (between 50 and 90 million) of transport aircraft by testing at high pressures (up to 4.5bar) and low temperatures (down to 110K). The dimensions of the test section are $2.4 \times 2.0$m. The length of the test section is 8.73m. The model is mounted on the ceiling of the chamber equipped with slotted side walls for half-model tests.

**Table 1.** ETW specification [5]

| | |
|---|---|
| Test section dimensions | $2.4 \times 2.0 \times 8.73$m |
| Mach number | 0.15–1.3 |
| Stagnation pressure | 1.15–4.5bar |
| Stagnation temperature | 110–313K |
| Max. Reynolds number | 50mln (full-span models) |
| Max. Reynolds number | 90mln (half-span models) |

The European Transonic Wind tunnel test chamber is a baseline facility for flow simulation of the DLR F11 model (see Figure 3).

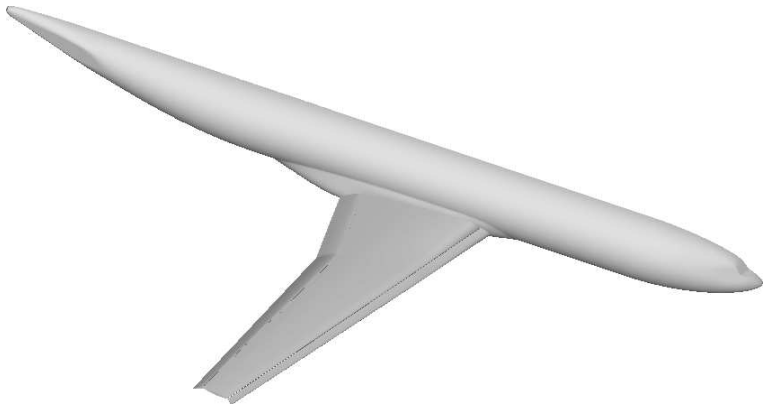

**Figure 3.** The DLR F11 model geometry

The DLR F11 model in high-lift landing configuration consists of a fuselage and a three-element wing (the main element, a full-span slat and a full-span flap). It has a length of approx. 3m, a half-span of 1.5m and a mean aerodynamic chord of 0.35m. The distance between the inlet plane and the point of model rotation (PMR) is 3.7m.

**Table 2.** Dimensions of the DLR F11 model

| | |
|---|---|
| Length | $\sim 3$m |
| Half-span | $\sim 1.5$m |
| Mean aerodynamic chord | $\sim 0.35$m |

Three model mounting strategies were investigated numerically. One reflects the full-span geometry with a mirror plane located at the centreline of the fuselage (Figure 4, left). Additionally, the half-model may be mounted directly at the wall (Figure 4, middle) or using a fully sealed peniche (Figure 4, right).

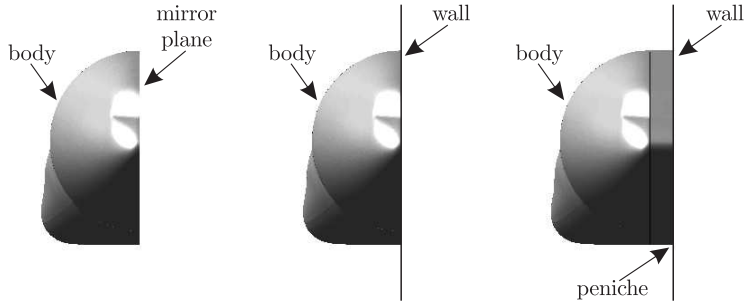


**Figure 4.** The DLR F11 fuselage mounting strategies

The main objective of the present study is to asses the influence of the peniche's height on the comparison of aerodynamic characteristics of full-span and half-span models.

A standard peniche used in the aircraft industry is non-metric – the forces exhibited on its surface are disregarded during the global lift and drag measurements. This means that both the model fuselage and the peniche have to be independent. The stand off-fuselage gap has to be properly sealed to avoid destructive transpiration flow.

## 3. The DLR F11 model in the ETW chimera mesh

The main idea of the chimera technique is to generate grids for complex configurations easily by decomposing them into simple, independent parts. The only limitation is that all component meshes should overlap with each other to allow inter-grid communication. All meshes are placed within a simple background Cartesian grid. If any grid volume lies inside a solid body of the neighbouring component grid, it is marked and excluded from the calculation process.

The project included four component chimera meshes placed in the background Cartesian tunnel grid (see Figure 5 and Table 3). It consisted of a fuselage mesh with or without a peniche (C-O type), slat, main and flap grids (all of the C type). The only difference between the three investigated configuration types (full-span, half-span model placed directly on the wall, and half-span model with a peniche) was the existence of clustering near the sidewall boundary layer and an additional layer of peniche blocks in this type of mounting.

The chimera technique allows relatively simple mesh generation for each component grid. Additionally, re-meshing of the whole model is not necessary when the angle of attack is changed. The rotation is done in FLOWer, only the relative position of the model and the wind tunnel grid are changed.

The component grids were created automatically using python scripts and the Numeca Interactive Grid Generator. There was a different, independent set of python scripts for each component. The scripts automatically loaded the geometry, performed

**Table 3.** The DLR F11 model's component grids

| | Number of blocks | Number of cells |
|---|---|---|
| Wind tunnel | 2 | 1.9–2.6mln |
| Fuselage and peniche | 8–14 | 2.3–7.2mln |
| Slat | 9 | 2.4mln |
| Main | 6 | 2.2mln |
| Flap | 6 | 1.3mln |

topology creation and generated surface and volume grids based on a set of user pre-defined parameters. Without automatic script-based grid generation different, peniche shapes would require manual re-meshing each time the geometry was changed. The development of the python scripts was the most time-consuming part of the research.

There are two kinds of wind tunnel grids. One is used for computations with a symmetry condition at the mirror plane of the model, reflecting a full-span computation. The other is equipped with boundary layer clustering at the wall where the half-model is mounted. Both configurations have a special inlet block with four Euler walls, designed to overcome the influence of the short distance between the inlet plane and the model. With this configuration, the upstream distance for boundary layer development is kept constant (3.7m), allowing the inlet plane to be moved freely. There is a non-matching connection between this block and the main tunnel block.

The fuselage grid has three configurations depending on the model mounting strategy. One is used for a full-span simulation, another for a half-model placed directly on the wall, and yet another for a half-model equipped with a peniche.

The three-element wing component meshes are common and independent of model mounting (see Figure 6).

To resolve the flow field accurately enough, one simulation of the whole aircraft model in a wind tunnel, for a certain angle of attack, Mach number, Reynolds number and peniche shape, requires a chimera mesh that consists of up to 16 million volumes.

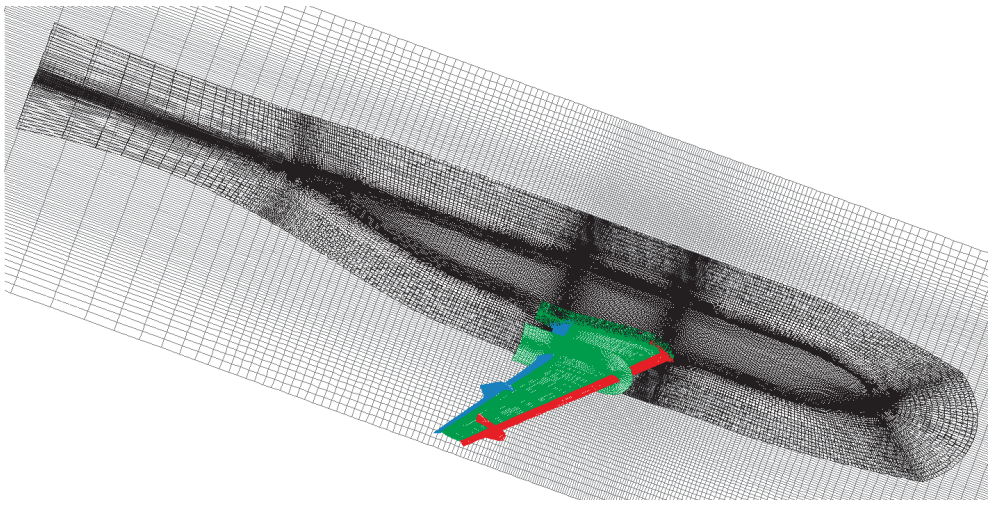

**Figure 5.** DLR F11 model chimera grid

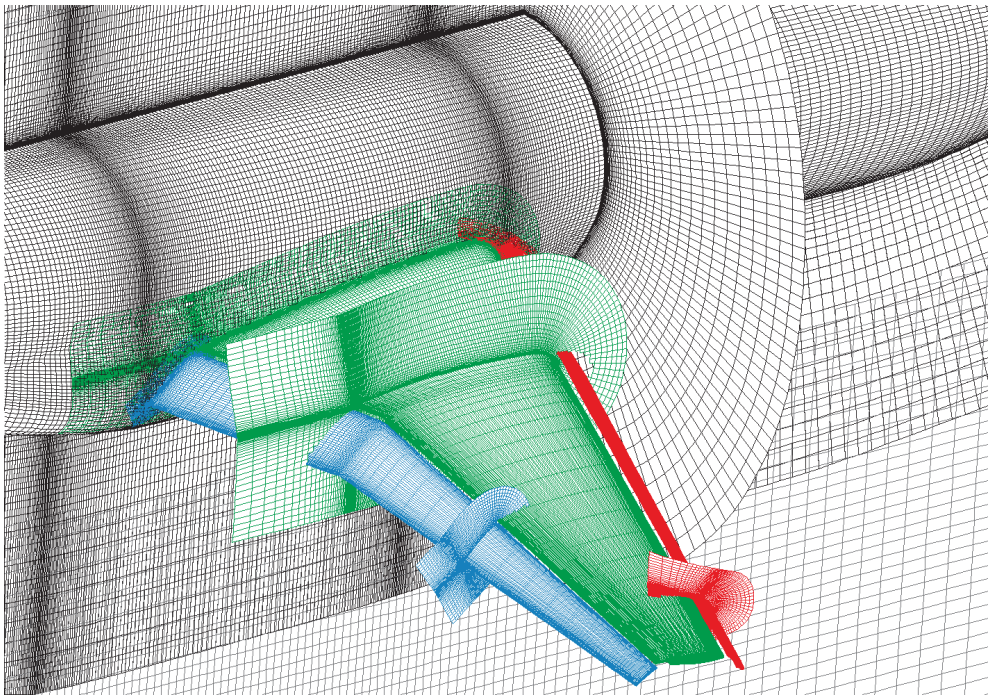

**Figure 6.** The DLR F11 model chimera grid: the wing area

**Table 4.** The DLR F11 model in the tunnel: grid details

| | Number of blocks | Number of cells | Memory consumption |
|---|---|---|---|
| Full-span | 31 | 10.1mln | 10.0GB |
| Half-span without a peniche | 31 | 12.6mln | 12.5GB |
| Half-span with a 30mm peniche | 37 | 15.6mln | 15.5GB |

This task consumes up to 16GB of RAM for a single run and needs relatively fast processors (see Table 4).

When using the chimera technique, it is necessary to minimize errors associated with the interpolation of flow variables between overlapping meshes. The FLOWer code points out all problematic points where interpolation failed with a value copied (instead of interpolated) from the nearest volume. For the DLR F11 model in the ETW tunnel project, the number of such inaccurate points has been less than 160, exclusively in the wing area. For complicated geometries it is very time consuming to avoid interpolation problems completely.

Six holes had to be constructed for the hole-cutting algorithm necessary for the chimera overlapping grids technique. These holes blank all volumes of each grid that lay inside a geometry of the model. The overlapping of component grids on the surface of the fuselage is clearly visible in Figure 7. All volumes of one component grid that lay inside other components are blanked. It is necessary to avoid unphysical computation of the flow inside the geometry.

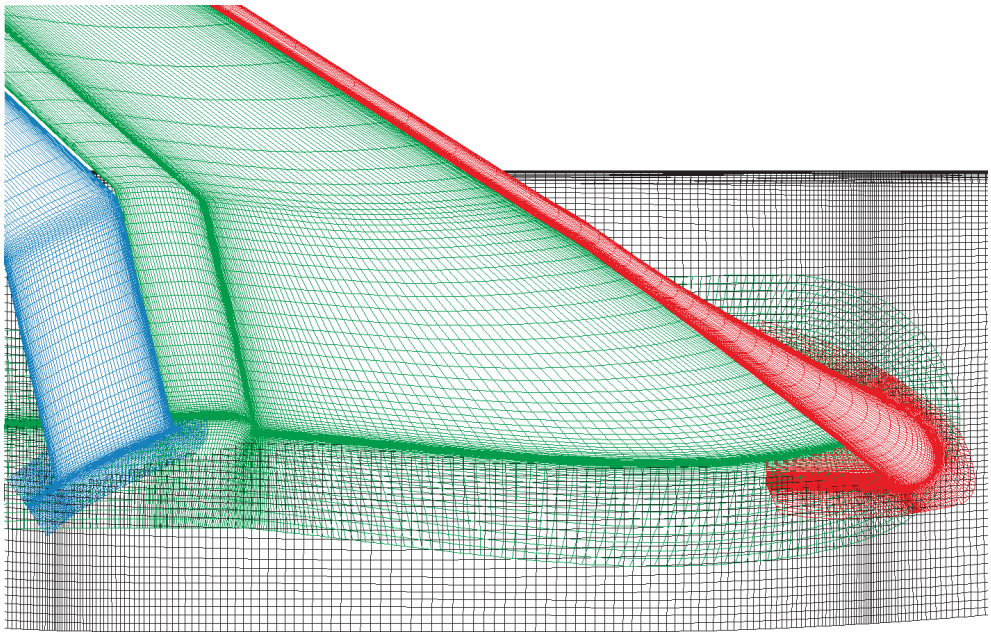

**Figure 7.** The DLR F11 model chimera grid: mesh overlapping on the fuselage surface

Because the chimera technique allows overlapping of more than one mesh on the surface of the body, a calculation of the aerodynamic forces acting on this surface may lead to incorrect predictions. Due to the existence of multiple volumes in one region on the surface, it is necessary to remove overlapping by creating a unique surface of the model. A special post-processing tool, Trisurf (DLR), removes overlapping on

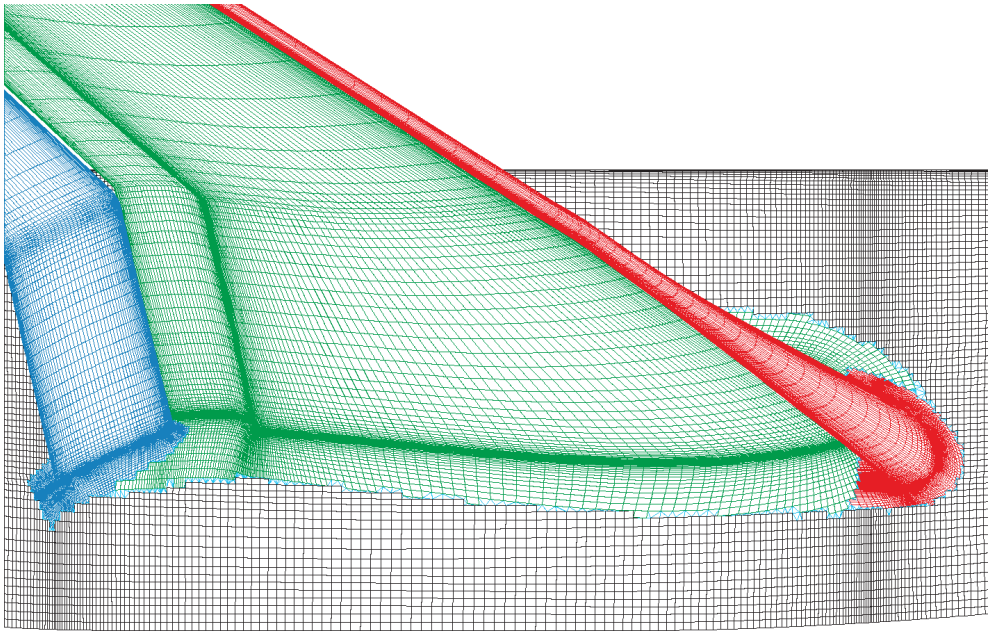

**Figure 8.** The DLR F11 model chimera grid: mesh overlapping removed from the fuselage surface

the surface and correctly calculates all aerodynamic forces acting on the model (see Figure 8).

## 4. Flow parameters and boundary conditions

A FLOWer flow solver from DLR, Germany, was used. It is a modern block-structured, finite volume code that solves Reynolds Averaged Navier-Stokes equations with various turbulence models (Table 5).

**Table 5.** Simulation details

| | |
|---|---|
| Grid generator | IGG (Numeca), python scripts |
| RANS solver | FLOWer ROT (DLR) |
| Post processing tool | Tecplot (Amtec), Trisurf (DLR) |
| Turbulence model | $k$-$\omega$ SST |
| Dissipation scheme | Jameson |
| Space discretization | finite volume, cell centred, $2^{\text{nd}}$ order |
| Time integration | 5 stage Runge-Kutta |
| Preconditioning | ON or OFF |
| Multigrid, multilevel | 3-level or less |
| CFL | 10.0 or less |
| Transition | fully turbulent |

The tunnel mesh had three Euler walls (a boundary condition simulating slotted ETW walls) and a Navier-Stokes no-slip wall. For some computations, the Navier-Stokes wall was interchanged with a symmetry plane boundary condition allowing simulation of the full-span model flow. Inlet and outlet conditions were set to obtain the desired Ma and Re number at these planes.

Navier-Stokes walls were set for the whole fuselage, peniche and wing surface. The only exceptions were blunt trailing edges of the slat, main, flap and body, where Euler walls were applied. Also the tip surfaces of all three wing elements were set to Euler walls.

All computations were performed for $\mathrm{Ma} = 0.155$ and $\mathrm{Re} = 15$ million. The angle of attack varied from $\alpha = -5^{\circ}$ to $\alpha = 25^{\circ}$. The half-model was equipped with a 30mm peniche. The reference temperature was set to $T_{inf} = 120\mathrm{K}$ and the reference Reynolds length equalled the model's mean aerodynamic chord, $c_{ref} = 347.09\mathrm{mm}$ (see Table 6). The inlet turbulence characteristics were chosen to equal the default values (free-stream turbulence intensity of 0.005 and the ratio of turbulent to laminar viscosity of 0.001).

**Table 6.** Flow parameters and boundary conditions

| | |
|---|---|
| Mach number | 0.177 |
| Reynolds number | 15mln |
| Reynolds length | 347.09mm |
| Temperature | 120K |
| Angle of attack | $-5^{\circ}$ to $25^{\circ}$ |
| Peniche height | mirror, 0, 30 |

## 5. Simulation results

The simulations began with a calculation of the flow in the empty ETW tunnel. The peniche's effectiveness is closely dependent on the incoming boundary layer shape. Usually the peniche's height is referenced to the boundary layer's height (or to displacement thickness) at the point of model rotation (PMR). In our case the boundary layer height was approx. 80mm at this cross-section (see Figure 9). The first peniche used was only 30mm high. The original peniche of ETW has 95.1mm and removes the model from the sidewall boundary layer completely.

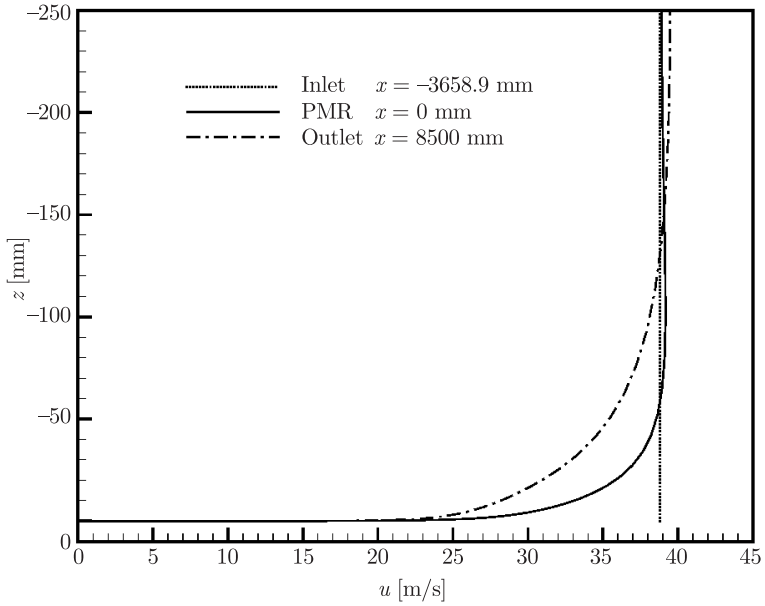


**Figure 9.** Empty tunnel boundary layers

Contour maps of pressure coefficient, $C_p$, are presented in Figures 10–12 for all three configurations: the full-span model (Figure 10), the half-span model mounted on the tunnel wall without a peniche (Figure 11) and with a peniche (Figure 12). The angle of attack is close to the maximum lift, $\alpha = 19^{\circ}$. A blue colour indicates areas of large flow acceleration while a red colour reveals low-speed regions. The sidewall pressure coefficient contour map is visible only when a sidewall boundary layer is present (*cf.* Figures 11 and 12).

The pressure coefficient, $C_p$, near the nose and in the whole area of the mirror plane is smeared by the incoming side-wall boundary layer (see Figures 11 and 12). The flow's acceleration on the fuselage near the wing-root is also greater for the full-span computation (see Figure 10); it apparently impacts the aerodynamic performance and forces acting on the model.

The half-span model computation with a 30mm peniche has revealed even greater differences than the full-span results (see Figure 12), especially in the nose region, influenced by the incoming boundary layer due to increased resistance to the incoming flow.

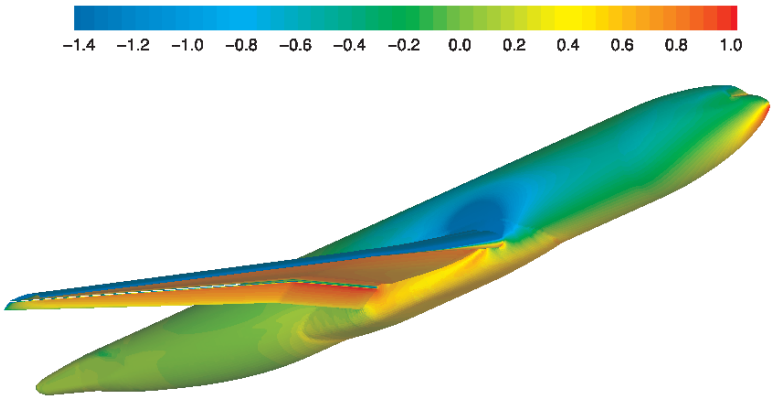


**Figure 10.** The DLR F11 full-span model: $C_p$ contour map, $\alpha = 19^\circ$

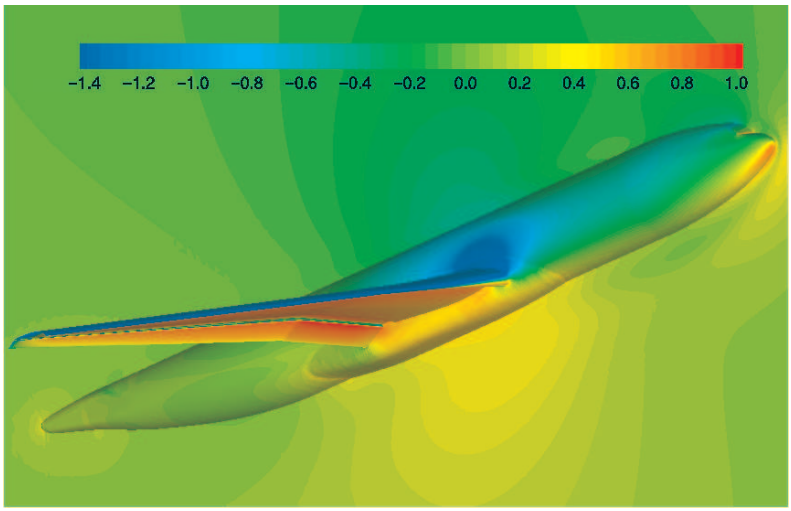


**Figure 11.** The DLR F11 half-span model without a peniche: $C_p$ contour map, $\alpha = 19^\circ$

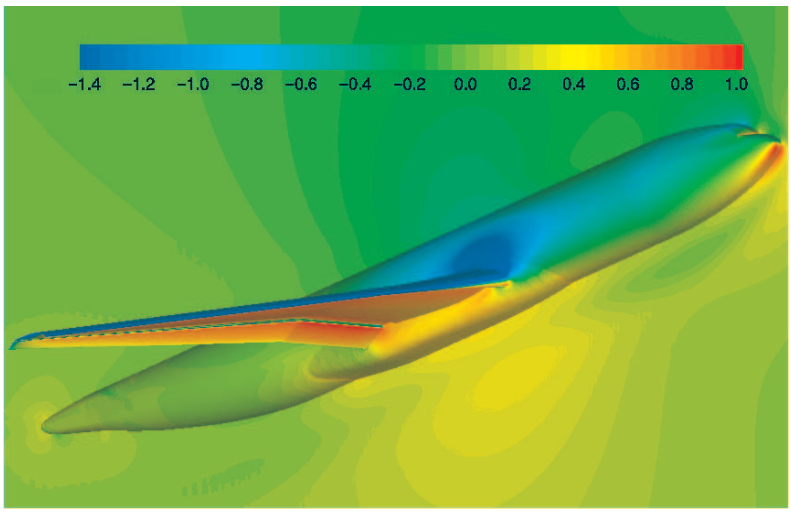


**Figure 12.** The DLR F11 model with a peniche: $C_p$ contour map, $\alpha = 19^\circ$

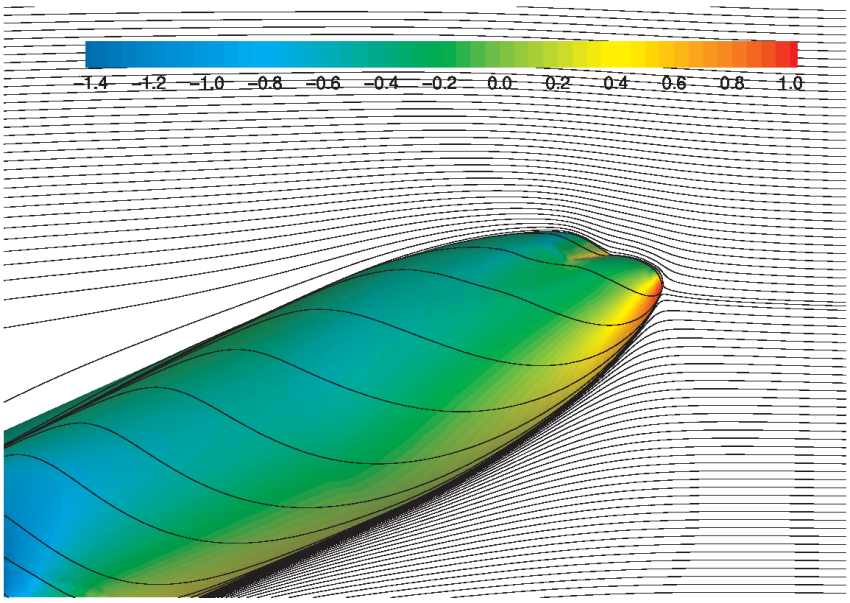


**Figure 13.** The DLR F11 full-span model:
$C_p$ contour map and stream lines, $\alpha = 19^\circ$

The change of the flow pattern is clearly visible in the stream-line visualization of the model's nose region (*cf.* Figures 13, 14 and 15).

The full-span computation with a symmetry boundary condition at the model's mirror plane exhibits the most desirable behaviour of the flow's stream line pattern (see Figure 13). When the half-model is mounted on the wall, directly or with

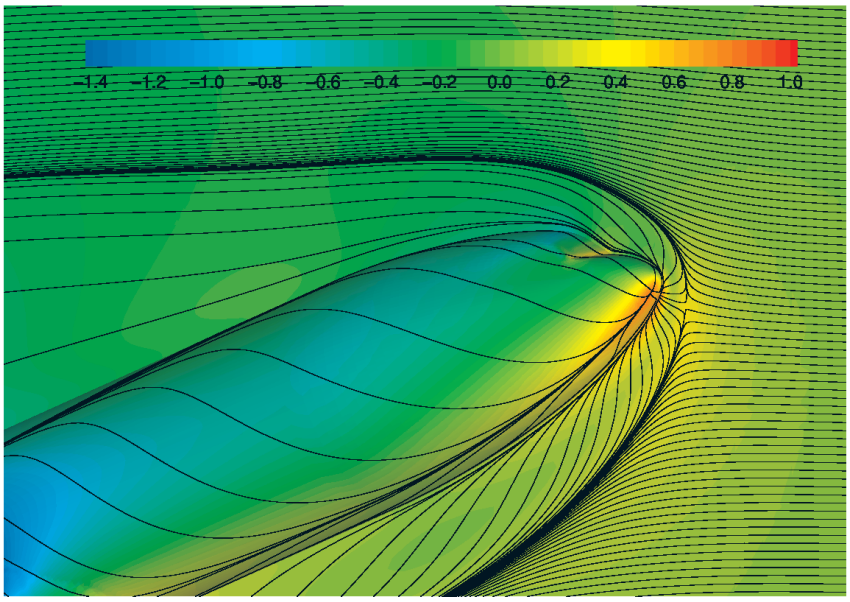


**Figure 14.** The DLR F11 half-span model without a peniche:
$C_p$ contour map and stream lines, $\alpha = 19^\circ$

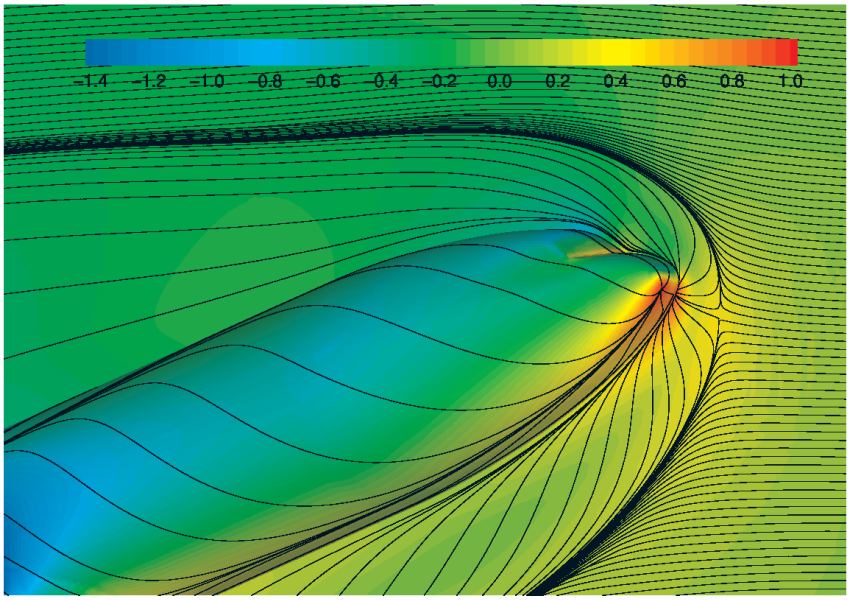


**Figure 15.** The DLR F11 half-span model with a 30mm peniche: $C_p$ contour map and stream lines, $\alpha = 19^{\circ}$

a peniche, a vortex is formed at the model's nose (see Figures 14 and 15). The boundary layer separates upstream of the peniche and rolls up to form a horse-shoe vortex in the junction region.

The application of a 30mm peniche increases the disturbance to the incoming boundary layer and the strength and size of the horse-shoe vortex (see Figure 15). In comparison with the half-model mounted on the wall without any additional peniche, the separation line is shifted further upstream. It is worth mentioning that the side plane used for stream-line visualization of the half-span model equipped with a 30mm peniche was different from that of the other configurations, as the model's symmetry plane was no longer equal to the tunnel's side wall but was shifted by a distance equal to the peniche's height.

A comparison of contour maps of the pressure coefficient, $C_p$, for $\alpha = 19^{\circ}$ (*i.e.* close to the model's maximum lift) reveals only minor differences between full-span and half-span without a peniche configurations (see Figure 16). First computations with the angle of attack increased beyond the maximum lift ($\alpha > 19^{\circ}$) have shown a constant trend of increasing difference.

Greater differences in surface $C_p$ contour maps occur when a half-model is mounted on a 30mm peniche (see Figure 17). Surprisingly, this computation is in poorer agreement with the full-span data than a half-span calculation with a model mounted directly on the wall.

The greater the distance from the centreline of the model, the lesser the influence of the mounting strategy on the wing pressure distribution (*cf.* Figures 18 and 19). A wing $C_p$ in the cross-section very close to the wing-body junction is presented in Figure 18. The acceleration near the leading edge of all elements on the upper surface varies depending on the type of mounting. The full-span flow indicates

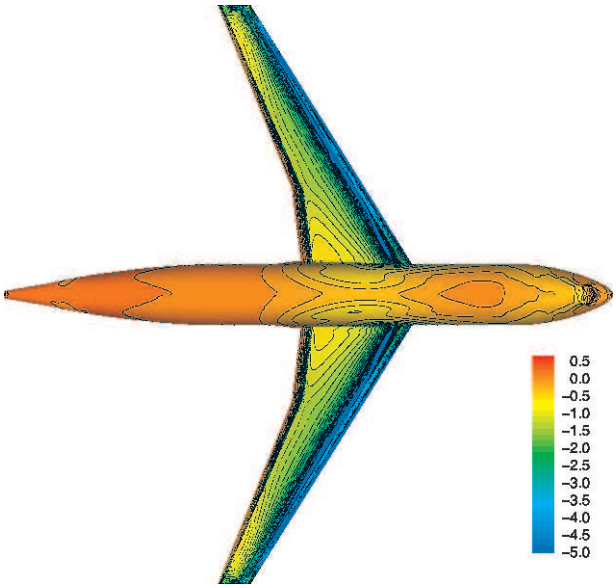


**Figure 16.** The DLR F11 full-span (lower half) and half-span without a peniche (upper half) models: $C_p$ contour map comparison, $\alpha = 19^\circ$

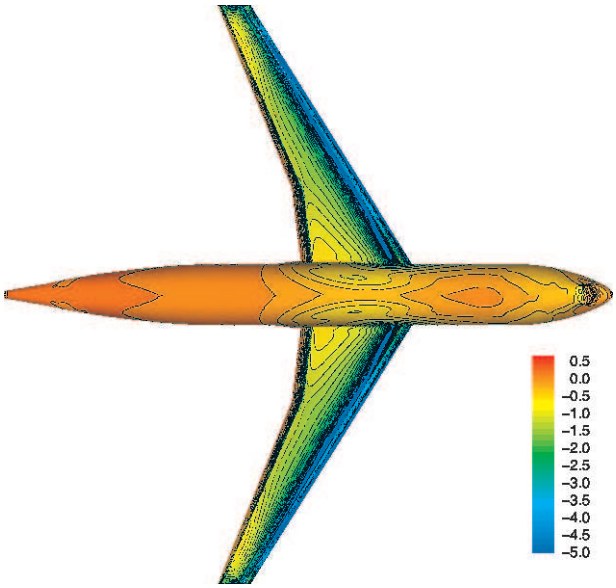


**Figure 17.** The DLR F11 full-span (lower half) and half-span with a 30mm peniche (upper half) models: $C_p$ contour map comparison, $\alpha = 19^\circ$

a drop in pressure (and acceleration) different than that of the half-span geometries. In contrast, the lower-surface $C_p$ exhibits only minor differences.

A wing $C_p$ in the cross-section very close to the wing's tip is presented in Figure 19. The upper and lower surface $C_p$'s indicate only small differences due to the greater distance to the tunnel's side wall. This deviation is the most pronounced for the computation with a 30mm peniche, especially on the upper surface of the wing.

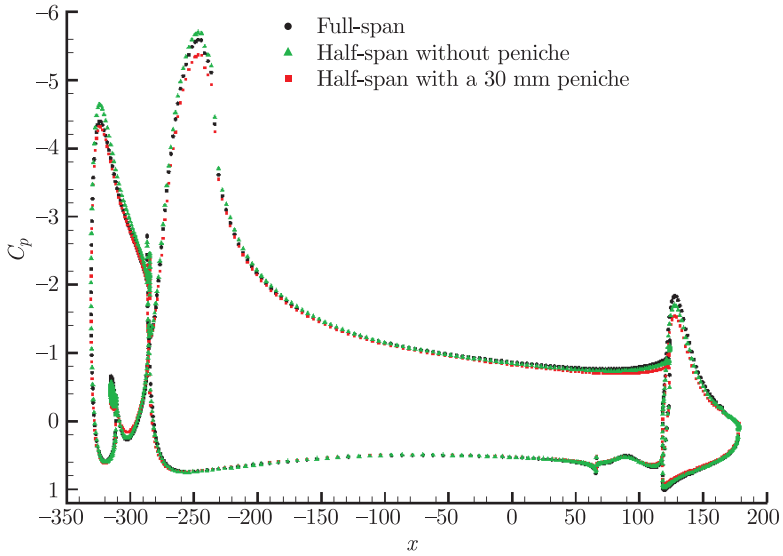


**Figure 18.** The DLR F11 wing $C_p$ distribution near the wing-body junction, $\alpha = 19^\circ$

However, a comparison of the aerodynamic performance of all the configurations based on lift, $C_L$, drag, $C_D$, and the moment coefficient, $C_M$, is the most important (see Table 7). Surprisingly, the larger the peniche, the worse the comparison with the full-span data. The best match with the full-span computation has been found for the fuselage mounted directly on the wall (*i.e.* peniche height of 0mm), for both angles of attack ($\alpha = 0^\circ$ and $\alpha = 19^\circ$).

The relative differences between full-span and half-span configurations are presented in Table 8. The $C_L$ difference for the model without a peniche is $-1.0\%$, while application of the 30mm stand-off leads to a $+1.4\%$ difference for $\alpha = 19^\circ$. For

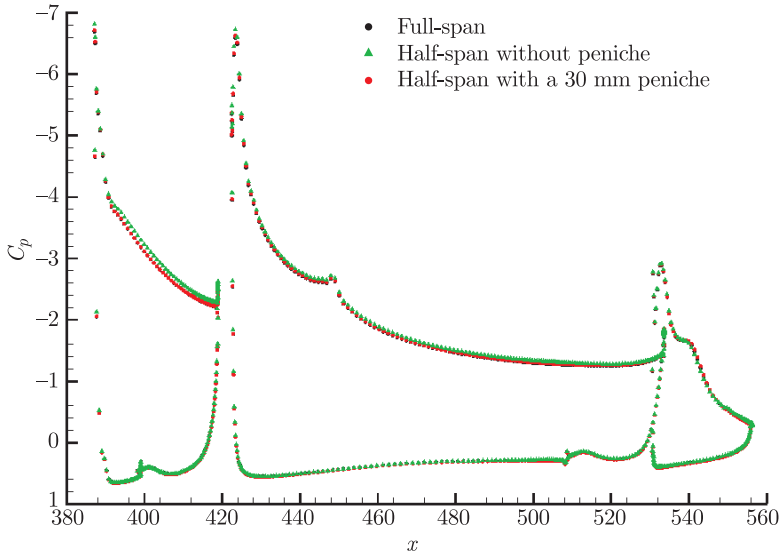


**Figure 19.** The DLR F11 wing $C_p$ distribution near the tip of the wing, $\alpha = 19^\circ$

**Table 7.** Aerodynamic coefficients: Ma = 0.177, Re = 15 mln

| | $\alpha$ [°] | $C_L$ | $C_D$ | $C_M$ |
|---|---|---|---|---|
| Full-span | 0 | 1.4340 | 0.09360 | 0.63491 |
| | 19 | 2.7307 | 1.2862 | 0.44443 |
| Half-span without a peniche | 0 | 1.4352 | 0.09451 | 0.63603 |
| | 19 | 2.7040 | 1.2732 | 0.44870 |
| Half-span with a 30 mm peniche | 0 | 1.4450 | 0.09357 | 0.63931 |
| | 19 | 2.7677 | 1.2870 | 0.41940 |

**Table 8.** Difference in aerodynamic coefficients: Ma = 0.177, Re = 15 mln

| | $\alpha$ [°] | $\Delta C_L$ [%] | $\Delta C_D$ [%] | $\Delta C_M$ [%] |
|---|---|---|---|---|
| Full-span | 0 | 0 | 0 | 0 |
| | 19 | 0 | 0 | 0 |
| Half-span without a peniche | 0 | +0.1 | +1.0 | +0.2 |
| | 19 | −1.0 | −1.0 | +1.0 |
| Half-span with a 30 mm peniche | 0 | +0.8 | −0.03 | +0.7 |
| | 19 | +1.4 | +0.1 | −5.6 |

$\alpha = 0^\circ$ the differences are quite small. The influence of the mounting strategy increases with increasing angle of attack.

## 6. Conclusions and future work

Preliminary computations of the DLR F11 model were carried out in the ETW tunnel geometry in full-span and half-span without and with a 30 mm peniche configurations, for angles of attack $\alpha = 0^\circ$ and $\alpha = 19^\circ$. Surprisingly, a comparison of their aerodynamic performance has revealed that the best match with full-span data is obtained for a model mounted directly on the wall, without the addition of a 30 mm peniche. This observation has to be verified for angles of attack beyond the maximum lift, where visible differences tend to increase. It is possible that a smaller peniche height ($< 30$ mm) would produce better result.

Interestingly, relative differences in aerodynamic coefficients calculated from the computational results with a fully sealed peniche are very small ($\Delta C_L < 1.5\%$). Usually, deviations in $C_L$ measured experimentally under high-lift conditions between full-span and half-span models are of the order of 10%–15% for angles of attack close to the maximum lift. This suggests that there is another factor responsible for such behaviour in the experiment, possibly the sealing between the non-metric peniche and the half-model fuselage. Therefore, a new peniche configuration should be prepared and computed including an effective gap between the peniche and the DLR F11 fuselage.

### *Acknowledgements*

The work has been performed under the HPC-EUROPA Project (RII3-CT-2003-506079), with the support of the European Community – Research Infrastructure Action under the FP6 "Structuring the European Research Area" Programme.

### *References*

[1] Milholen W E and Chokani N 1996 *Computational Analysis of Semi-span Model Test Techniques*, NASA Contractor Report 4709

[2] Gatlin G M and McGhee R J 1996 *Study of Semi-span Model Test Techniques*, AIAA 96-2386
[3] Milholen W E and Chokani N 1996 *Development of Semi-span Model Test Techniques*, AIAA 96-2412
[4] Gatlin G M, Parker P A and Owens L R Jr 2001 *Development of a Semi-span Test Capability at National Transonic Facility*, AIAA 2001-0759
[5] Gross N and Quest J 2004 *The ETW Wall Interference Assessment for Full and Half Models*, AIAA 2004-0769